Enhancing Solid State Carbon Quantum Dot Solar Cells by Manipulating the TiO_2 Electron Transport Layer

A Major Qualifying Project

Submitted to the Faculty of

Worcester Polytechnic Institute

in partial fulfillment of the requirements for the

Degree in Bachelor of Science

in

Chemical Engineering

By

_____

Lucas Gagne

_____

Xandria Korn

_____

Alexander Rockcress

April 22, 2019

Project Advisors:

_____

Professor Michael Timko, Chemical Engineering

_____

Professor Pratap Rao, Mechanical Engineering

Abstract

Solar energy is a growing source of sustainable energy. However, some of the main components of solar cells are made up of inorganic, toxic, and expensive materials.[1, 2] In this study, carbon quantum dots (CQDs) were used as the photo-absorber in solar cells. CQDs are made from common organic carbon sources such as glucose, citric acid, and ethanediamine, and act as the semiconductor in a solar cell.[3, 4] The downside of CQDs in solar cells is their low efficiencies (<1%), whereas most modern solar cells produce efficiencies of around 20%. This study used the in-situ growth of CQDs onto the electron transport layer (ETL) of a solid state solar cell through hydrothermal carbonization. By testing cells with varying ETLs, it was found that decreasing the ETL thickness increased efficiency.

Table of Contents

Abstract 2
Table of Figures 5
Table of Tables 5
Introduction 6
Background 7
Solar Cells 7
Quantum Dots 8
Previous Experiments 10
Mesoporous Titanium Oxide Layer Characteristics 11
Methods 12
General Overview 12
Preparing Plates for HTC 12
Materials 12
Cutting and Cleaning the FTO Glass 12
Compact Titanium Oxide Layer 13
Mesoporous Titanium Oxide Layer 13
Hydrothermal Carbonization Reaction 14
Building the Cell 15
CuSCN Transport Layer General Solution Procedure 15
CuSCN Transport Layer Application Method 1 15
CuSCN Transport Layer Application Method 2 15
CuSCN Transport Layer Application Method 3 15
Gold Plating 16
Electric Potential Testing 17
Raman Spectroscopy 17
Results and Discussion 18
CQD Solar Cells' Photovoltaic Efficiencies 18
Effect of Varying CuSCN Application Method 20
Scanning Electron Microscopy (SEM) Images 20
RAMAN Spectroscopy 22
Sources of Error 23

m-TiO_2 application 24
CQD Application 24
HTC Crucible Contamination 24
Gold Plating 24
Testing 24
Conclusion 25
Reccomendations 26
References 27
Appendix 29
Appendix A: Drawing of FTO Plate Holder Base 29
Appendix B: Exploded View of Plate Holder Assembly 30
Appendix C: Example Calculation for PCE 31
Appendix D: Photovoltaic data 32
Appendix E: Sample Methods and Corresponding Efficiencies 35
Appendix F: SEM Images of Samples 1 and 2 36
Sample 1 Before CQDs 36
Sample 1 After CQDs 37
Sample 2 Before CQDs 38
Sample 2 After CQDs 39

Table of Figures

Figure 1: Solar Cell Components 7
Figure 2: CQD Solar Cell Configuration 16
Figure 3: Photovoltaic Results for Samples 1, 2, 13, and 16 18
Figure 4: Sample Photos and Calculated % Efficiencies 19
Figure 5: SEM Images of Sample 1 21
Figure 6: SEM Images of Sample 2 22
Figure 7: Raman spectroscopy of various samples 23

Table of Tables

Table 1: Characteristics of m-TiO_2 Layer on Samples 14
Table 2: CuScn Method for Each Sample 15

Introduction

Since the first solar cell was created in 1941 by Russell Olh,[5] the concept of solely using solar energy as an energy source has saturated the collective human mind and remains on the forefront of the goal towards a sustainable future, along with nuclear and wind energy. Even though solar energy is on the forefront of the clean energy initiative, there is much to expand upon to improve their capabilities. Solar cells of the past have been made efficiently, yet with less desirable materials: gallium, arsenic, bismuth and sulfur, to name a few. These semiconductor materials can be costly, toxic, and non-renewable.[2] The average lifespan of these cells is 20 years, without a chance of recycling the raw materials inside.[6]

Recently, a new direction has been taken to alleviate these non-renewability issues by creating solar cells from carbon and nitrogen sources, such as carbon quantum dots (CQDs).[7] Some of these tests used elements of ethanediamine, chitin, glucose, and citric acid. As carbon and nitrogen sources are extremely abundant in nature (found in sugar, ethanol, amino acids, etc) the effective use of them in solar cells would prove incredibly beneficial towards the goal of sustainability.

While still in the early theoretical stage of existence, carbon based solar cells are gaining much traction in in the scientific field from their feasibility. These CQD based solar cells are very new in modern science and they do show some initial difficulties, such as the low efficiencies they produce.

This study is intended to provide further insight into how to increase the efficiency of these CQD solar cells. There are two novel approaches to tackle changing the efficiency: by creating solid-state CQD solar cell and by manipulating the hole transport layer of the solar cells. These test were performed in the chemical and mechanical engineering departments of Worcester Polytechnic Institute. Each of the cells that were produced were run through SEM imaging, electric potential testing, and raman spectroscopy.

Background

Solar Cells

Solar cells provide access to a powerful and reliable renewable source of energy, however current technology is still far behind capturing the 173,000 terawatts of energy the sun provides each day. This energy produced by the sun is 10,000 times more than the total energy usage of the world.[8] Solar cells, also commonly called photovoltaic (PV) cells, directly convert sunlight into electricity through material properties that causes them to release electrons when photons of light are absorbed. The electrons released by a semiconductor can be absorbed by silicon or other materials that can easily carry charge. The proton and electron absorption layers create an electric field that forces the flow of electrons creating usable energy. An example of the layer of a cell can be seen in Figure 1.

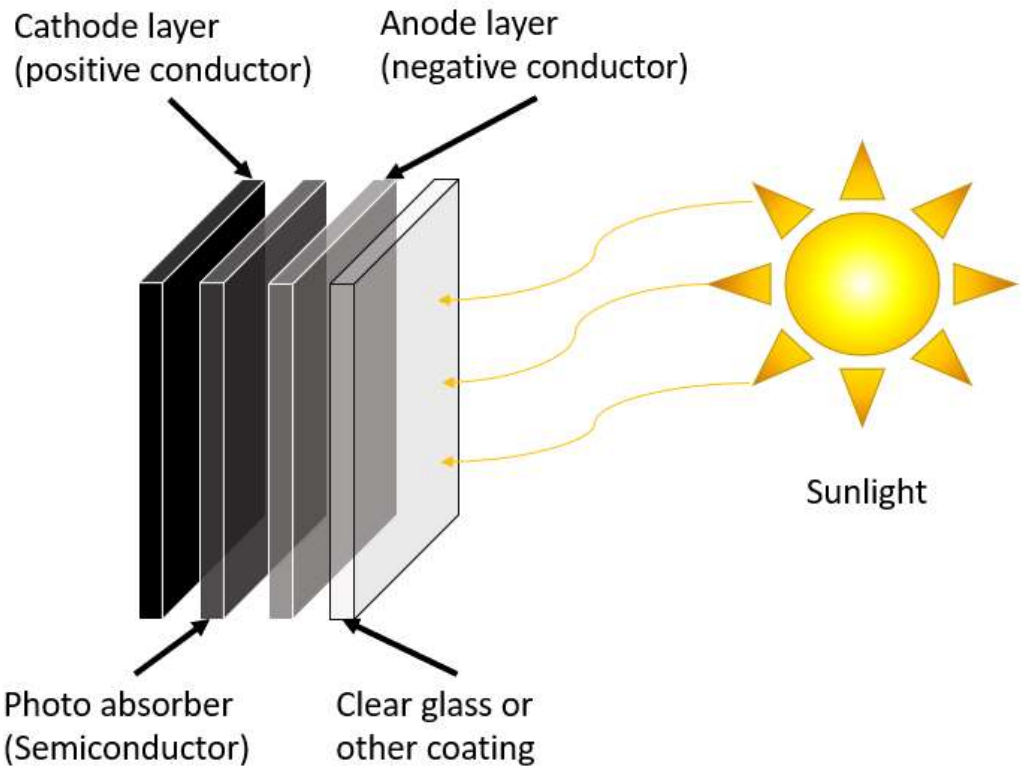

Figure 1: Solar Cell Components

Harnessing the sun's energy through solar cells has great benefits for the world. Solar energy is easily accessible in many regions including space. In the 1960's, it began to be used to provide power aboard spacecraft. Since that time solar panels have started to gain recognition as a useful source of renewable energy.[9] The use of solar cells benefits the environment by reducing the carbon footprint generated from fossil fuels and replacing many energy sources with the renewable energy from sunlight. In 2017, 71.5 million metric tons of CO_2 were saved from solar and wind renewable energy.[10] Solar cells result in minimal pollution of any kind and could slow down the rate at which harmful emissions, such as nitrous oxides, enter the atmosphere.[11]

Although solar cells have a lot of benefits there are many drawbacks to implementing them. Most solar cells have low conversion efficiency meaning that most of the energy that hits the cell in the form of light is not converted into usable energy.[12] Cells that have higher conversion come at a higher manufacturing cost such as silicon cells.[13] Even with a high conversion solar cell the energy produced is a small percent of the energy provided by the sun. Solar cells also have the disadvantage of only being able to produce energy during the day when skies are fairly clear. Solar cells require large amounts of space and can only be spread horizontally taking up land that could have been used for other things. Energy produced when not being sent straight to the grid requires a separate storage space. Furthermore, many materials in current solar cells used are toxic and are often not properly handled when creating and disposing of the panels. This increases pollution of water, soil, and air in many areas.[1]

Quantum Dots

Quantum dots are heteroatomic molecules that have high photoluminescent properties and semiconductor-like qualities (in many cases, they are semiconductors). The main types of quantum dots that have been studied are heavy metal semiconductors, graphene quantum dots, and carbon quantum dots.[14] Being heavy metals, they are synthesized with different organic or inorganic compounds (sulfur, nitrogen, selenium, arsenic, gallium, indium, etc.).

Recently, carbon quantum dots (CQDs) have gained popularity in the research and development fields of science. CQDs are organic molecules that have great electrocatalytic, photoluminescent, and electroluminescent potential. CQDs are nanostructured heteroatomic molecules that high versatility in application, low toxicity, simple synthesis, and high renewability.

It is important to note the differences and similarities between inorganic quantum dots and CQDs. The previous holder of the term "quantum dots" are heavy metal semiconductors. However, these are expensive and highly toxic to the environment.[2] CQDs are similar to other quantum dots due to the physicochemical properties that define quantum dots. The way that quantum dots operate is through the interactions of the atoms; ionic and covalent bonds show the highest activity for electron transport. This phenomenon will work in favor for the use of carbon quantum dots as a substitute semiconductor.

There are many ways of synthesizing carbon quantum dots. Such methods are microwave radiation, Electrolysis, and hydrothermal carbonization (HTC). Microwave radiation is very fast method of CQD synthesis. Being one step and scalable, this provides a very economical method of CQD synthesis.[15] One of the drawbacks of microwave radiation assisted pyrolysis is that there is poor control over the sizes of resultant carbon quantum dots (poor uniformity of sizes).

Electrolysis can be used for synthesizing a graphene-specific CQD. This method requires the passing of a current through an electrolytic solution.[15] Originally this was done with graphene rods as both the anode and cathode in an ethanol/NaOH solution. Graphene quantum dots are a type of CQD that relies on the structured nature of sheet graphene. It allows high conductivity of electrons through its apparatus.

HTC is a reliable, low cost method to create carbon quantum dots.[18,19] Biomass and other organic compounds are heated in reactor to between 150 and 350ºC to produce a solid carbon product. However, at temperatures about 250ºC, hydrothermal liquefaction reactions begin to compete with HTC. This carbon product, also referred to as char, can contain as much as 80% of the carbon initially in process. This char product is more hydrophobic than the starting material. Water is an important medium for HTC and allows for the reactions that produce char.[16] Along with water the reaction is often assisted by solvents or microwave irradiations.[18,19] For Hydrothermal reactions, acidic water favors the formation of char and reduces competing reactions. HTC allows for high production of solid carbon char that has many potential uses.[16]

Finally, the in situ growth of CQDs directly applies the CQDs to the surface of the metal that is used as the base of the solar cell.[4] There is minimal research into this method; however, the experiments that have been carried out with this method have had exceptional results in quantum yield, power conversion efficiency, and economics, far more so than the other methods that have yields in the same categories. It seems logical that this was done, as previous methods included the pyrolysis of the CQD solution, this single step method improved almost every aspect of CQD use. By allowing the metal backbone to be submersed in the solution while it was being pyrolyzed, the CQDs formed over the surface of the backbone in their own unique order.

Carbon quantum dots have a very high renewability attribute. CQDs are made from all sorts of carbon sources. This is truly a benefit to the research and development of carbon-based solar cells because there are carbon rich sources all over the world, and they can be found anywhere from the carbon in waste to the carbon that is found in the trees in forests to the carbon that is in shells of sea creatures.

While carbon commonly has very weak luminescence, CQDs show a very strong presence of photoluminescence.[3] This allows them to be very versatile for photonics, optics, and sensing in biometrics. Carbon Quantum dots have a very high solubility in water. This allows them to be very beneficial to uses in the medical field and in environmental sensory fields.

Though CQDs boast some very enticing attributes, they are not without their drawbacks. One of the foremost problems of the application of CQDs is the power conversion efficiency (PCE) of the solar cells that it produces. CQDs are not as efficient in photovoltaic cells as inorganic semiconductor cells are. Inorganic semiconductors are much more efficient in solar cells for a number of reasons, some of which being size (electron distance of traversal) and conductibility.[17] The synthesis of CQDs can be simple yet often very laborious. The common problems that arise are as follows: carbonaceous aggregation, size control and uniformity, and surface properties.[3] Carbonaceous aggregation is the char that occurs from combusting organic compounds. It is not entirely carbon quantum dots. The most common CQDs that appear have a size in range of 6 - 8 nm, whereas the char left over from combustion can leave particles that range from 2 - 10 nm, which is not optimal for this process, and in many cases the other particles have no use. Finally, the surface properties of each particle will affect how efficient the whole cell is, from the concentration of quantum dots to how sterically hindered they are.

The method used in this study will be conducted through the experimental method of in situ growth of CQDs onto the TiO_2 layer of a solar cell. A series of similar experiments of CQD application will be conducted using different carbon sources applied to TiO_2 backbone. By allowing FTO glass to be suspended in solution of the carbon source and performing HTC, the CQDs grow directly on the TiO_2.

Previous Experiments

Although research on CQDs is still in the early stages, there have been a handful of experiments conducted that have advanced the understanding of how to maximize the effect of CQDs. To improve the effectiveness of a solar cell, the power conversion efficiency (PCE) must be improved. With the use inorganic quantum dots, the PCE can be upwards of 10%.[17] The use of CQDs in solar cells have reached a maximum PCE of 0.87% as of June 2017.[4] This PCE was reached by harvesting the growth of CQDs on the photoanode instead of soaking the anode in a solution of synthesized CQDs. This method will be used within this experiment.

In 2015, Briscoe compared PCEs of different CQDs all using a different base carbon chain.[7] The three CQDs compared in this experiment included chitin, chitosan, and D(+)-glucose based CQDs. Briscoe used ZnO nanorods for the anode. The PCEs of each trial were: 0.0004% for uncoated ZnO, 0.032% for chitin-based, 0.061% for chitosan-based, and 0.017 for glucose.

Furthermore, Margraf et al. found that increasing the acidity of the CQD solution increased the light absorbance of CQDs.[18] At a pH of 7 and 1, the absorbances were 0.8 and 1.4 respectively. Margraf et al. also studied the effect of anode soaking time to absorbance. They found that there is a great increase in absorbance over the first 10 hours. After 20 hours, there was minimal increase in absorbance over time.

Multiple studies have also been conducted on doping CQDs with other elements. The most common element used in CQD doping is nitrogen. Nitrogen-doped CQDs (NCQDs) have shown to improve the PCE of solar cells. In a 2013 study, Zhang produced NCQDs with a PCE of 0.13%, while non-doped CQDs produced a PCE of 0.03%.[19]

Compared to the heterogeneous aggregation of CQDs, in almost all the previous research done using CQDs, the homogeneous harvesting of CQDs on photoanodes is a novel concept. This study aims to use previous research on solar cells that use heterogeneous aggregation of CQDs and apply similar experiments on solar cells that use homogeneous harvesting of CQDs on solar cells.

Mesoporous Titanium Oxide Layer Characteristics

The mesoporous titanium oxide layer (m-TiO_2) is the last part of the photoanode layer. For this study, the characteristics of this layer were manipulated to optimize the PCE of the solar cell. The m-TiO_2 is the layer that the CQDs adhere to. The particle size and layer thickness of the m-TiO_2 effects how the cell performs.[25,26] A larger particle size will scatter more light, increasing PCE. However, larger particles result in less surface area for the CQDs to adhere to, decreasing PCE. Increasing the thickness of the m-TiO_2 layer will increase the surface area, but the layer will be harder for electrons to pass through. This study aimed to observe the effects of different m-TiO_2 layer conditions.

Methods

General Overview

The construction of the solar cells used in this study all followed the same general procedure. To start, fluorine-doped tin oxide (FTO) glass was cut and cleaned. Second, the compact titanium oxide (c-TiO_2) layer was applied to the conductive side of the FTO plate and annealed. Then, the mesoporous titanium oxide (m-TiO_2) layer was applied using a variety of experimental methods. The CQDs were then added to the prepared plates in-situ using an HTC reaction with an equimolar solution of ethane diamine (EDA) and citric acid as the reactants. After the plates were cleaned, a layer of copper thiocyanate (CuSCN) was added. Lastly, gold cells were placed on the prepared plates. Scanning electron microscopy (SEM) and potentiostat tests were completed to determine the characteristics and performance of the cells.

Preparing Plates for HTC

Materials

FTO glass was used as the base. The cleaning solutions included deionized water, acetone, and isopropyl alcohol. Titanium diisopropoxide (75% in propanol) and 1-butanol were used for the c-TiO_2 layer. The m-TiO_2 layer was made using two different kinds of TiO_2 pastes (depending on the sample) with ethanol as the solvent. For the earlier trials, a paste comprised of 20 nm particles was used. For the later trials, a paste comprised of 22 nm and >150 nm particles was used. Scotch tape was used to cover the FTO during the application of layer. It is recommended to use scotch tape that will easily come off the FTO glass without leaving any trace of adhesive on the surface.

Cutting and Cleaning the FTO Glass

To begin preparing the plates for HTC, the FTO glass must be cut to the desired size. For the plates to be able to fit in the custom apparatus made for HTC, the plates had to be no greater than 2.2 cm wide. A piece of each plate was cut off before HTC so that the TiO_2 layers could be studied under SEM before CQD were applied. Because of the extra cut before HTC, the glass plates were prepped at 2.5x2.5cm each. To save time during the application of the c-TiO_2 layer, one large plate (5x5cm) was used and cut into 4 equal parts after applying the c-TiO_2 layer. Using a diamond blade and running pliers on the nonconductive side of the FTO glass, a 5x5cm square was cut.

After cutting a 5x5cm section of FTO glass, the plate was cleaned to ensure that there were no contaminants that could inhibit the flow of electrons or light through the cell. The cleaning process started using a solution of 1:1:1 deionized water, acetone, and isopropanol. The plate was sonicated in this solution 3 times for 5 minutes each. After each repetition, the plate was rinsed with DI water. Lastly, the plate was sonicated using 100% isopropanol for 10 minutes. The plate was dried using compressed air, completing the cleaning process.

Compact Titanium Oxide Layer

To begin the application of the c-TiO_2 layer, two mixtures were made: a 0.15M TiO_2 solution and a 0.30M TiO_2 solution. The solutions were made by dissolving titanium diisopropoxide (75% in propanol) in 1-butanol. The 0.15M TiO_2 solution called for 0.055mL of titanium diisopropoxide and 1mL of 1-butanol. The 0.30M solution called for 0.110mL of titanium diisopropoxide and 1 mL of 1-butanol.

First, the cleaned FTO glass was taped on opposite ends, covering about 0.5 cm on both sides. The 0.15M TiO_2 mixture was pipetted onto the conductive side of the FTO glass, covering the entire area, and spin-coated for 30 seconds at 2000 rpm and 1000 rpms. The tape was removed, and the plate was annealed for 5 minutes on a 125ºC hot plate. The plate was then taped again, and spin-coated at the same settings using the 0.30M TiO_2 solution. After annealing for 5 minutes at 125ºC, the plate was spin-coated again using the 0.30M solution. Lastly, the plate was annealed in an oven at 500ºC for 30 minutes, completing the application of the c-TiO_2 layer. Annealing the plate ensured that all of the solvent was evaporated and the c-TiO2 layer was adhered to the glass properly.

Mesoporous Titanium Oxide Layer

For each sample, the m-TiO_2 layer was made using TiO_2 paste dissolved in ethanol. The following factors were manipulated in this study: type of paste, weight percent of paste in ethanol, application method, and number of layers. The parameters for each sample are described in Table 1.

Two different pastes were used in this study. One paste had a particle size of 20 nm and the other had 22 nm particles and >150 nm particles. The paste solution was applied to the glass plate by either spin coating or doctor blading.

For the spin-coated layers, the bare FTO on the plate was taped so that only the part of the plate with c-TiO_2 was exposed. The paste solution was then dropped onto the plate, covering the entire surface, and spin-coated at 4000 rpm and 1000 rpms for 30 seconds. For the samples that had multiple layers, the plate was then annealed on a hot plate at 125ºC for 10 minutes so that the paste would adhere to the plate before adding another layer. The paste was then spin-coated again and annealed on the hot plate until the desired number of m-TiO_2 layers were applied.

For the doctor-bladed samples, the bare FTO on the plate was taped. The opposite side was also taped, partially covering the c-TiO_2 layer. The two pieces of tape acted as a guide for spreading the paste solution, while also determining the thickness of the m-TiO_2 layer. The paste solution was then dropped on the plate (about 0.15 mL) and spread using the side of a glass pipet. The plate was left to dry for about 1 minute before removing the tape.

After the m-TiO_2 layer was applied using either spin coating or doctor blading, they were annealed in an oven at 500ºC for 1 hour, completing the m-TiO_2 layer.

Table 1: Characteristics of m-TiO_2 Layer on Samples

Sample	Type of Paste	Weight % of Paste/Ethanol	Application Method	Layers
1	25 nm	50/50	spin-coated	1
2	25 nm	50/50	spin-coated	2
3	25 nm	50/50	spin-coated	1
4	25 nm	50/50	spin-coated	2
5	25 nm	50/50	spin-coated	1
6	25 nm	50/50	spin-coated	2
7	25 nm	50/50	spin-coated	3
8	25 nm	50/50	doctor-bladed	1
9	25 nm	50/50	spin-coated	1
10	25 nm	50/50	spin-coated	2
11	25 nm	50/50	spin-coated	3
12	25 nm	50/50	doctor-bladed	1
13	20 nm and >150 nm	20/80	spin-coated	1
14	20 nm and >150 nm	50/50	spin-coated	1
15	20 nm and >150 nm	20/80	doctor-bladed	1
16	20 nm and >150 nm	50/50	doctor-bladed	1

Hydrothermal Carbonization Reaction

To proceed with HTC, the reactor was loaded with 4 plates in a holder designed to keep the plates vertical during the reaction process. Drawings of the holder can be found in Appendix A and B. The plates were placed vertical in a symmetric way so that the CQD layer would be more uniform and consistent. After the plates were loaded into the reactor we made the 100mL of 0.5M Citric acid and 0.5M EDA in DI water. This molar ratio was taken from Zhang's study on in situ growth of CQDs on solar cells.[1] The capacity of our reactor was 100 mL which left enough room for some expansion as the reactor was heated to minimize the chance of damage from pressure to the reactor. After adding the solution to the reactor the sealed reactor was then placed in the oven and heated to 180 C for 24 hrs. After this time the oven was turned off and allowed to cool for 12 hours. After removing the plates they were rinsed with DI-water then sonicated for 5 minutes in DI-water. The rinsing and sonication in DI water serve to remove carbons that are not strongly bonded to the TiO2.

Building the Cell

CuSCN Transport Layer General Solution Procedure

To build the a solid state cell for testing a CuSCN transport layer was next added to the plate. Two make this layer first a 40mg CuSCN and 1 mL diethyl sulfide solution was mixed for two hours at 60 C. The mixed solution was then filtered with a 0.2 μm filter. Three methods to apply CuSCN solution to the cell were tested to produce the best transport layer and improve productivity of the cell. The corresponding samples tested with each method can be seen in Table 2.

CuSCN Transport Layer Application Method 1

For the first method of application 35 μL of solution was placed onto the plate before spin-coating. The machine was then run at 500 RPM and 100 RPMS for 60 seconds. After this the plate was annealed for 10 minutes at 65ºC. This allows for a uniform coating of CuSCN and allows the solution to dry before adding the gold layer.

CuSCN Transport Layer Application Method 2

The second method of application used 35 μL of solution drop casted while the plate was spinning at 5000 RPM and 1000 RPMS. This was spun for about 30 seconds after drop casting to dry the plate and produce uniformity.

CuSCN Transport Layer Application Method 3

The third method of application started with soaking the plate in diethyl sulfide for 12 hours. This was followed by drop casting CuSCN solution onto the plate, making sure to cover the whole plate with solution before spin coating the plate at 500 RPM and 100 RPMS for 60 seconds.

Table 2: CuScn Method for Each Sample

CuSCN Method 1	CuSCN Method 2	CuSCN Method 3
Sample 3	Sample 1	Sample 9
Sample 4	Sample 2	Sample 10
Sample 5		Sample 11
Sample 6		Sample 12
Sample 7		Sample 13
Sample 8		Sample 14
		Sample 15
		Sample 16

Gold Plating

After the CuSCN layer each plate was then covered in foil with three 1 cm by 0.3 cm holes on the uniform CQDs. These covered plates were then placed in a thermal evaporator and gold coated. Each of the gold sections formed their own cell acting as the cathodic layer for the CQD solar cell. An example of the complete cell can be seen in Figure 2.

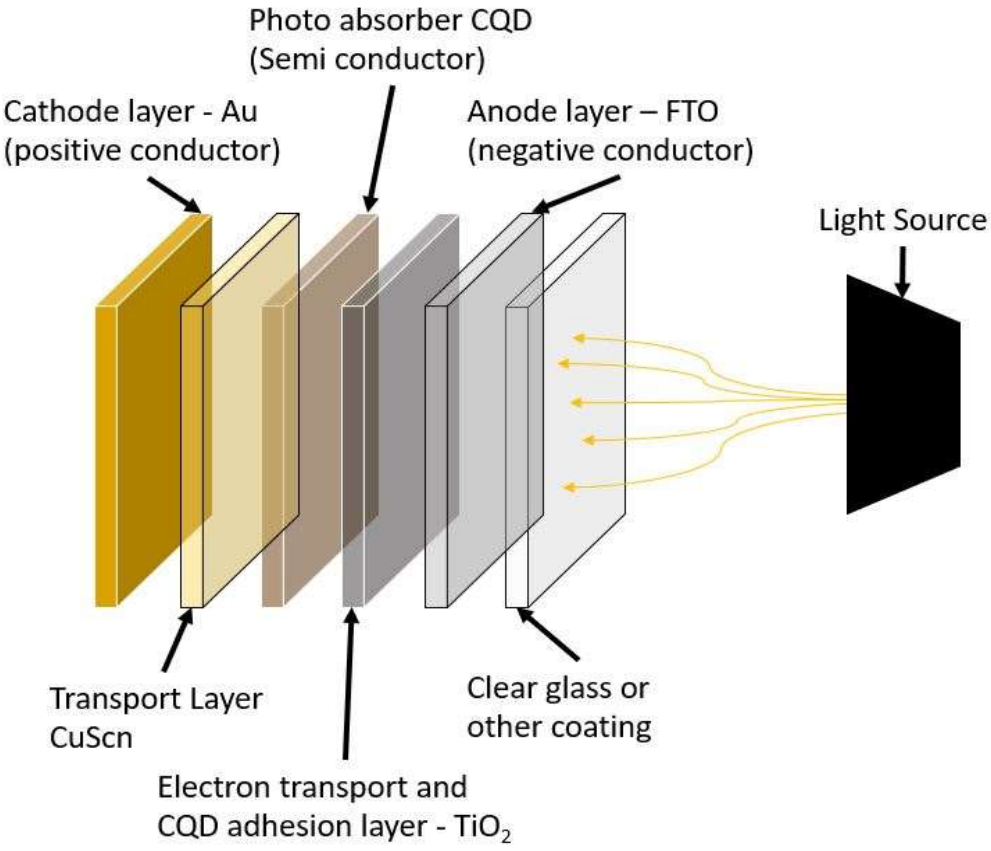

Figure 2: CQD Solar Cell Configuration

Electric Potential Testing

After the cells were built onto the prepared plates, the electric potential was tested using a potentiostat and a Newport SA2 Series xenon solar lamp. This test recorded the current at a range of voltages. From this, power was plotted against voltage and the efficiency was calculated using Equations 1 and 2.

$$\eta = \frac{P_{max}}{P_{inc}} \tag{1}$$

$$P_{max} = x_{mp} * V_{mp} \tag{2}$$

Where η is the efficiency and P_{inc} the power coming from the light source. P_{max} is defined by the greatest product of current (I_{mp}) and voltage (V_{mp}) at a single point. A more detailed calculation can be found in Appendix C.

Raman Spectroscopy

After the electric potential testing, small samples of plates ranging from our worst to best were through a raman spectrometer. A beam of green light was shot at a our cell in varying spots with varying strength of light. This test was performed to determine the chemical composition and consistency of our cell. This test performed much like an infrared spectrometer; it measured relative strength of reflection to the wavelength of light.

Results and Discussion

CQD Solar Cells' Photovoltaic Efficiencies

Photovoltaic experiments immediately show if a solar cell has any energy capabilities and are used to calculate efficiency of a solar cell which is a common comparison for solar cells. As seen in Figure 3 below photovoltaic results for our samples varied drastically. In Appendix D, photovoltaic results for all samples tested can be found including graphs for cells that did not result in energy capabilities. Figure 3 demonstrates the three working types of curves we found in our samples. Although these samples do not have chopping for each working plate we did run a test with light chopping. The drops to 0 mA when no light was applied proved the sample was working because of the light and that the baseline current was 0 mA meaning that the samples current at each voltage was due only to the absorbtion of light.

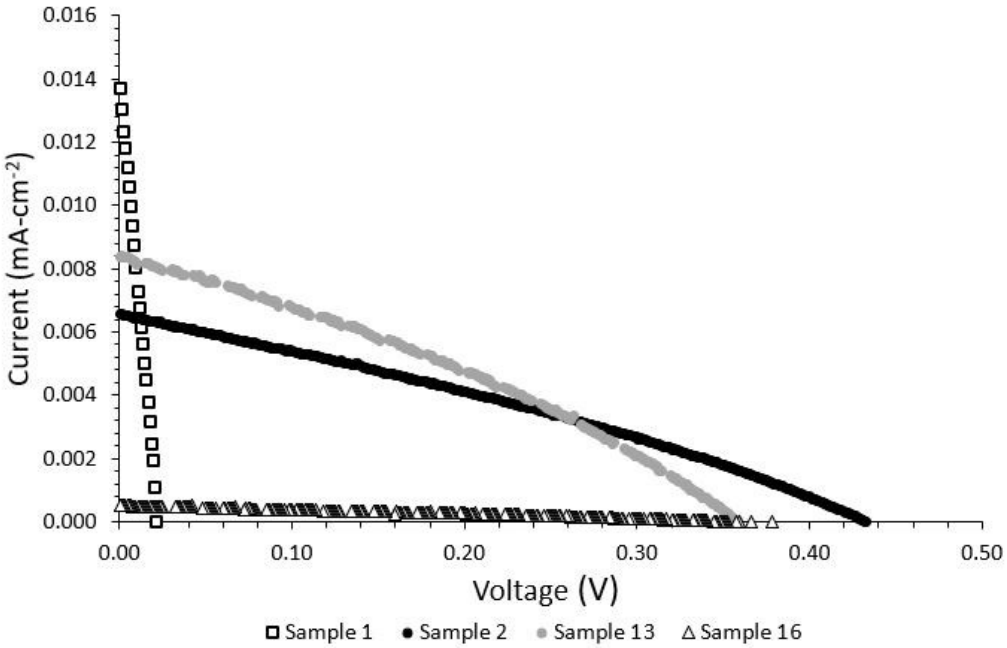

Figure 3: Photovoltaic Results for Samples 1, 2, 13, and 16

Sample 1 had a high maximum current however it did not produce current at higher voltages resulting in an overall low cell efficiency. Sample 16 was the exact opposite producing current at a high voltage but never reaching a high current which again resulted in a low solar cell efficiency. Samples 2 and 13 produced two of the three best efficiencies of the cells tested. These cells can be seen below to produce a curve in the voltage range of 0 to 0.5 which is ideal for producing the maximum efficiency. Figure 4 shows each sample and its maximum efficiency. Appendix E shows all of the methods and efficiencies for each sample.

Figure 4: Sample Photos and Calculated % Efficiencies

The cell efficiencies prove two important factors. The first factor is that it is possible to create solar cells using the proposed in-situ CQD growth method proposed by previous research.[4] The second factor is that although an increased thickness of the TiO_2 layer does visually increase the CQD adhesion factor, this increase thickness does not increase efficiency at the tested thicknesses. Particle diameter and CuSCN methods have an inconclusive affect on the 16 samples tested.

Effect of Varying CuSCN Application Method

All three methods of applying CuSCN onto the solar cell worked in producing a working cell. The three top performing samples (2, 4, and 13) all used different CuSCN methods, showing that the method of CuSCN application had little to no effect on the PCE of the samples. However, with the limited amount of data points, more test could be done to confirm this conclusion.

Scanning Electron Microscopy (SEM) Images

Using an SEM machine, images of the top and front cross section were taken of plates 1 and 2 at up to 70,000 times zoom. Images of these plates were taken before and after the addition of the CQD layer. The purpose of this test was to identify if the CQDs could be visually seen on the plates. Figure 5 and Figure 6 shows the SEM images of plates 1 and 2 before and after the addition of CQDs.

From the cross section images, there are three distinct layers. The bottom layer, which is about 400 nm thick, is the FTO layer. Following this layer (about 100 nm thick) is the compact TiO_2 layer. The final layer seen (2 - 5 μm thick) is the mesoporous TiO_2 layer. The m-TiO_2 layer on sample 1 around 5 μm thick, whereas sample 2's m-TiO_2 layer is about 2 μm thick. This was expected because sample 1 had two layers of m-TiO_2 paste spin-coated on and sample 2 had 1 layer of m-TiO_2 paste spin-coated on. From the cross section pictures, it is hard to determine where the CQDs are or what they look like. However, the images that include CQDs seem to have more roughness to the m-TiO_2 layer, which could be the cause of the CQDs. A similar phenomenon is shown in the top view images. The m-TiO_2 layer before the addition of CQDs had larger particles with less uniformity compared to the images after the CQDs were added. There was not a comparable difference between the top views of sample 1 compared to the top views of sample 2.

Sample 2 had a higher efficiency than sample 1. This is probably the fault of the m-TiO_2 layer thickness. The large distance that an electron would have to travel in sample 1's 5 μm layer would make it difficult for electrons to pass though compared to sample 2's 2 μm thick layer.

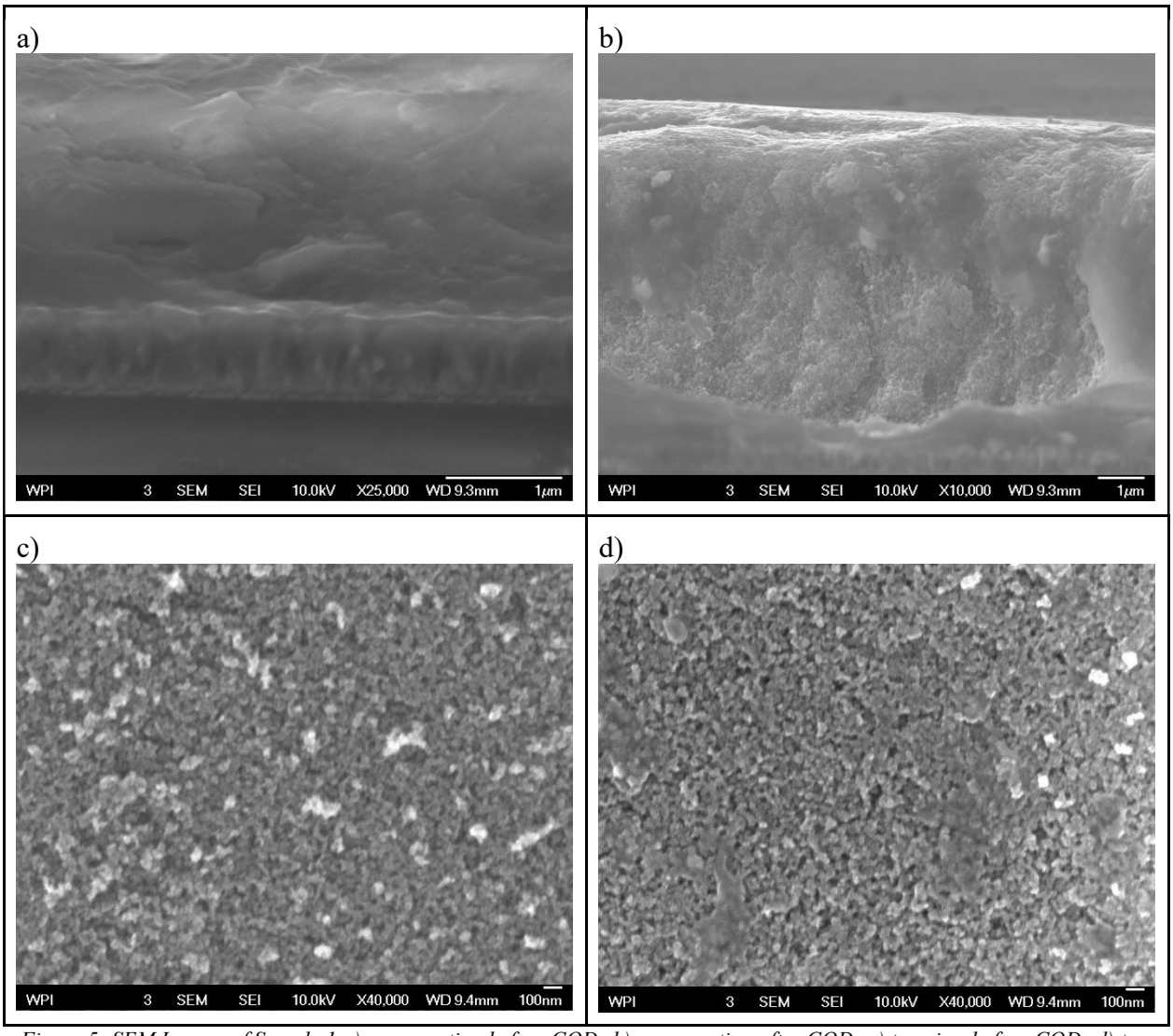

Figure 5: SEM Images of Sample 1 a) cross section before CQDs b) cross section after CQDs c) top view before CQDs d) top view after CQDs

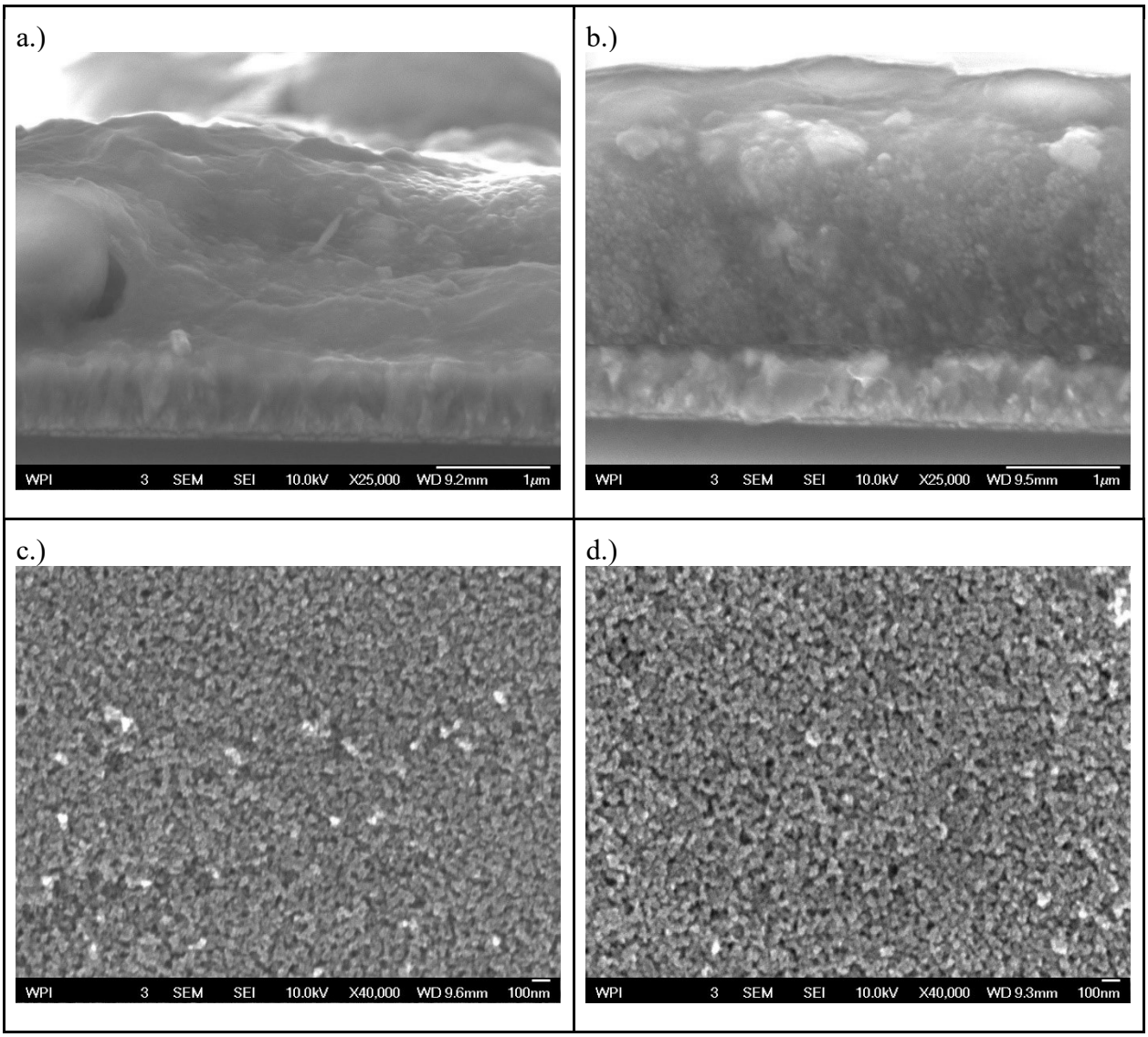

Figure 6: SEM Images of Sample 2 a) cross section before CQDs b) cross section after CQDs c) top view before CQDs d) top view after CQDs

All SEM images of samples 1 and 2 can be found in Appendix F.

RAMAN Spectroscopy

The purpose of running the raman spectroscopy tests was to confirm the composition of the plates and to see if there was a trend between the compositions and cell efficiency. Figure 7 shows the raman spectroscopy data from cells 4, 5, 9, and 13 at 10% light intensity. Samples 4, 5, and 9 were chosen because they all had the same m-TiO_2 application method but different efficiencies. Sample 13 was chosen because it used a larger particle diameter m-TiO_2 paste. The series of peaks at 140, 380, 510, and 640 corresponds with TiO_2. The peaks at 1320, 1400, and 1580 corresponds with carbon. The peak at 2165 corresponds with CuSCN.

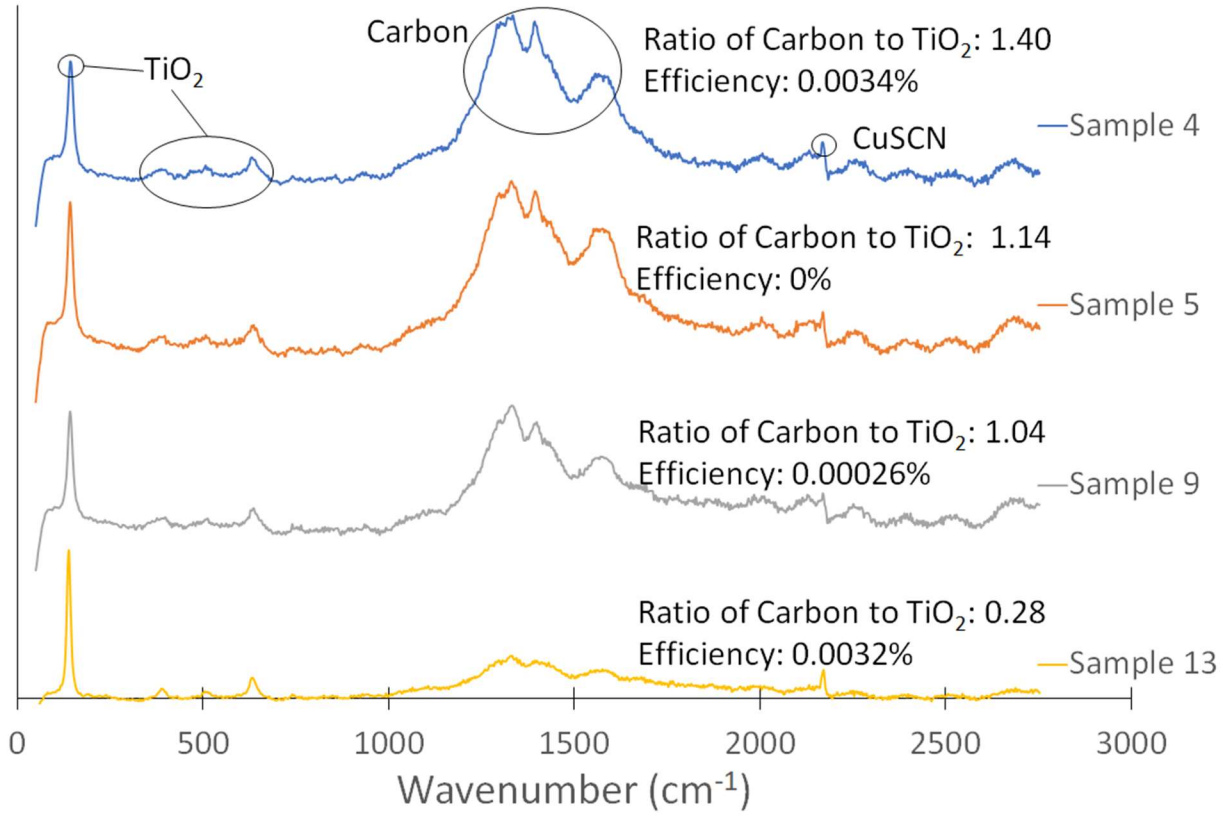

Figure 7: Raman spectroscopy of various samples

To compare the plates, the ratio between the peaks at 1320 (carbon) and 140 (TiO_2) were calculated for each plate. It was believed that there would be a trend between the ratio of carbon to TiO_2 and the cells efficiency. Since samples 4, 5, and 9 all had the same application method of TiO_2 (same amount of TiO_2), it was hypothesized that the sample with more carbon (or CQDs) would produce a better efficiency. However, there was no trend found. The ratio of carbon to TiO_2 values were similar for samples 4, 5, and 9 (1.40, 1.14, and 1.04 respectively), but the efficiencies were not (0.0034, 0, 0.00026% respectively). Furthermore, sample 13 had the lowest ratio of carbon to TiO_2 (0.28) but performed better than almost all the cells in efficiency (0.0032%). This could be due to the varying TiO_2 particle diameters in the paste used for sample 13.

Sources of Error

In each of the methods used to create and test the cells, there is error introduced, which is to be expected. In this study, only the quality and total error of the cells can be supposed and qualified, and not readily quantified. In a chronological order, the error of each of the steps are as follows.

m-TiO_2 application

In this step, varying amounts of mesoporous TiO_2 was spin-coated. The goal was to have a uniform surface of m-TiO_2 in order to attain uniform CQD distribution. According to the SEM images of samples, there was a wide range of uniformity in the cells varying from minimal disturbance in the consistency of TiO_2 to a high non-uniformity. Thus, it is assumed that the error is, on average, moderate in the grand effect of overall cell efficiency.

CQD Application

In this step, hydrothermal carbonization (HTC) was performed usicng carbon and nitrogen sources at 180ºC for 24 hours, with a 12 hour cooldown. HTC was performed in an oven with a maximum of four cells per run in the 0.5 M EDA and 0.5 cirtic acid. It was not possible to mix the solution while the experiment was running, so the solution may not have been entirely uniform in concentration. However, upon viewing the cells after the CQD deposition with cells of different thicknesses of m-TiO_2, it seemed that a linear correlation of the darkness of the cell (CQD discoloration) with the increase of of the m-TiO_2 layer, thus we assumed this to be a minor source of error.

HTC Crucible Contamination

Because HTC was operated in a shared laboratory, there were others who used varying carbon sources in the crucible for HTC for their own various experiments. The error that stems from this source would come from residual carbon in the teflon container, which would expand and contract upon heating and cooling, trapping carbon sources in the walls. This was alleviated as much as possible by cleaning the crucible with DI water and acetone a minimum of two times in succession before each use. The error from this was assumed to be minimal.

Gold Plating

In this step, gold coatings were placed on each of the cells for the anode layer. The placings of these gold coatings were decided by a manner of equivalent spacing. The error source here is that the gold should be covering uniform layers of CQD's, CuSCN and TiO_2, however, it was very difficult to determine whether or not this alignment was achieved and could be a large source of error in the overall efficiency of the cell.

Testing

In the final step of testing the cell, a probe was placed to specific locations on the gold and a probe was placed to the cells exposed FTO glass. During testing, the gold on the cells would become displaced by the probe moving around and possible disturbances to the surfaces on which the probes and cells were placed, occasionally scratching the gold off. This was determined to be a moderate source of potential error.

Conclusion

Overall, applying CQDs in situ onto a solid state solar cell did produce a working cell. The highest efficiency of the cells tested in this study was 0.0034%. This is considerably lower than the 0.87% efficincy achieved in precious research.[4] It was orignally hypothesized that increasing the m-TiO_2 layer would increase the amount of surface area for CQDs to reside on, increasing the overall efficincy. However, the thicker layer m-TiO_2 cells tested preduced little to no efficiency. This is most likley the fault of the m-TiO_2 layer being too thick (around 5 μm) for electrons to pass through easily. Furhtermore, it was expected that having more carbon relative to TiO_2 would produce a better efficincy. However, based on raman spectroscopy data, there was no trend in the ratio of carbon to TiO_2 and cell efficiency. Cell 13, which had the second highest efficiency (0.0032%), had the least amount of carbon to TiO_2 with a ratio of 0.28. Cell 2, which had a similar efficiency (0.0034%) had a ratio of carbon to TiO_2 of 1.14. This is probably due to the different particle sizes of m-TiO_2 in cell 13 (22 nm and >150 nm). The increased and diversified particle diameters used in sample 13 may make it easier for CQDs to attach to the m-TiO_2, while still being thin enough for electrons to pass through easily.

The use of CQDs as the semiconductor layer of solar cells proves to be inexpensive, environmentally friendly, and renewable. Replacing toxic materials for organic materials in solar cells is a novel concept with minimal research conducted so far. With the expanding research in solar and renewable energy, CQD-based solar cells could have a key role in solving these energy problems.

Reccomendations

Moving forward, there are many directions that this study can be directed in. The improvisation of the uniformity of m-TiO_2, c-TiO_2 and CuSCN layers can only be improved in minimal amounts with the current spin coating method used. However, the CQD application and composition can be improved.

Through a thorough study of how various carbon sources and their relative molar ratios interact as a functional CQD, it is theorized that altered cell efficiencies will be found and maximized. In addition, a study of how the reaction kinetics of each source at varying temperatures work, this will hopefully provide less char and residual carbon while producing far more CQD's.

For CQD solar cells, the futher manipulation of the m-TiO_2 layer (by decreasing the bulk thickness and increasing the particle diameter and diversity in size) will be of benefit to the research. Potentially an ideal ratio can be found of thickness layer to average particle diameter.

References

1. Solar Energy Disadvantages: The Top Drawbacks of Solar Power. *https://www.renewableresourcescoalition.org/solar-energy-disadvantages/* (accessed Oct 28, 2018).
2. A Toxicologic Review of Quantum Dots: Toxicity Depends on Physicochemical and Environmental Factors. *Environmental Health Perspectives* **2006***, 114*, 165-172
3. Wang, Y.; Hu, A. Carbon quantum dots: synthesis, properties and applications. *Journal of Materials Chemistry C* **2014***, 2*, 6921-6939.
4. Zhang, Q.; Zhang, G.; Sun, X.; Yin, K.; Li, H. Improving the Power Conversion Efficiency of Carbon Quantum Dot-Sensitized Solar Cells by Growing the Dots on a TiO2 Photoanode In Situ. *Nanomaterials (Basel)* **2017***, 7*.
5. Solar panel history and overview - Energy Matters - the solar experts
6. Life cycle assessment of solar PV based electricity generation systems: A review A.F. Sherwani, J.A. Usmani , Varun
7. Briscoe, J.; Marinovic, A.; Sevilla, M.; Dunn, S.; Titirici, M. Biomass-Derived Carbon Quantum Dot Sensitizers for Solid-State Nanostructured Solar Cells
8. Top 6 Things You Didn't Know About Solar Energy. *https://www.energy.gov/articles/top-6-things-you-didnt-know-about-solar-energy* (accessed Oct 28, 2018).
9. Knier, G. How do Photovoltaics Work? *https://science.nasa.gov/science-news/science-at-nasa/2002/solarcells/*.
10. U.S. Energy-Related Carbon Dioxide Emissions, 2017. *https://www.eia.gov/environment/emissions/carbon/*.
11. 2018 Health & Environmental Benefits of Solar | EnergySage. **2017**.
12. Solar Performance and Efficiency. *https://www.energy.gov/eere/solar/articles/solar-performance-and-efficiency* (accessed Oct 28, 2018).
13. Photovoltaic (Solar Electric). */initiatives/photovoltaic-solar-electric* (accessed Oct 28, 2018).
14. Ying Lim, S.; Shen, W.; Gao, Z. Carbon quantum dots and their applications. *Chemical Society Reviews* **2015***, 44*, 362-381.
15. Raz Jelinek *Carbon Quantum Dots;* Springer Nature: Switzerland.
16. Biller, P., & Ross, A. (n.d.). Hydrothermal Carbonization. Retrieved from https://www.sciencedirect.com/topics/engineering/hydrothermal-carbonization

17. Conversion of sunlight to electric power by nanocrystalline dye-sensitized solar cells https://www.sciencedirect.com/science/article/pii/S101060300400108X.
18. T. Margraf, J.; Lodermeyer, F.; Strauss, V.; Haines, P.; Walter, J.; Peukert, W.; D. Costa, R.; Clark, T.; M. Guldi, D. Using carbon nanodots as inexpensive and environmentally friendly sensitizers in mesoscopic solar cells. *Nanoscale Horizons* **2016***, 1*, 220-226.
19. Yan-Qing Zhang; De-Kun Ma; Yan-Ge Zhang; Wei Chan; Xhao-Ming Huang N-doped carbon quantum dots for TiO2-based photocatalysts and dye-sensitized solar cells. **2013***, 2*, 545-552.
20. Jeng, M.; Wung, Y.; Chang, L.; Chow, L. Particle Size Effects of TiO Layers on the Solar Efficiency of Dye-Sensitized Solar Cells. International Journal of Photoenergy 2013, 2013.
21. Lee, Kim, Kim, Kim, Lee, Choi, . . . Joshi. (2017, November 16). Effect of TiO 2 particle size and layer thickness on mesoscopic perovskite solar cells. Retrieved from https://www.osti.gov/pages/servlets/purl/1414065

Appendix

Appendix A: Drawing of FTO Plate Holder Base

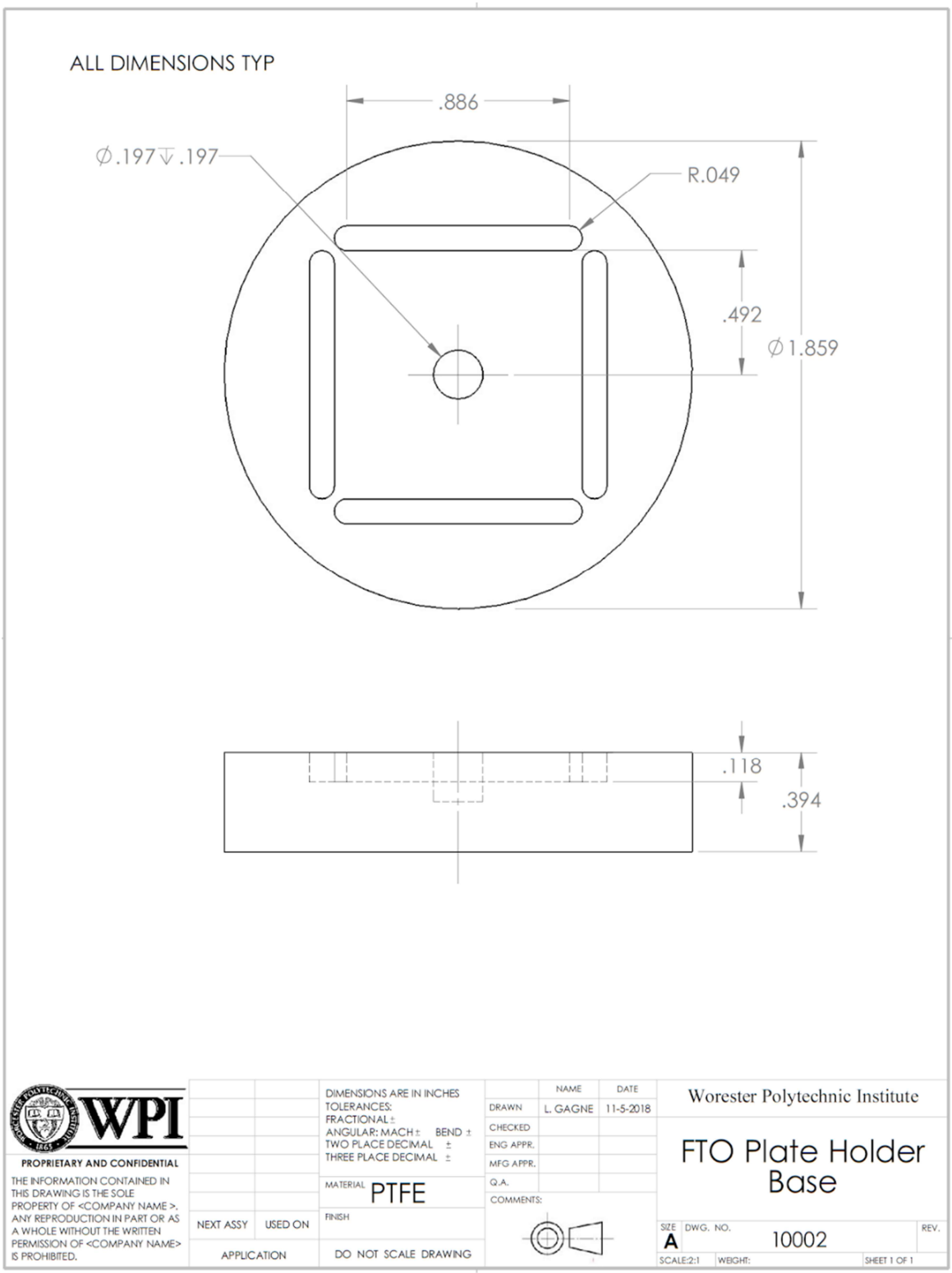

Appendix B: Exploded View of Plate Holder Assembly

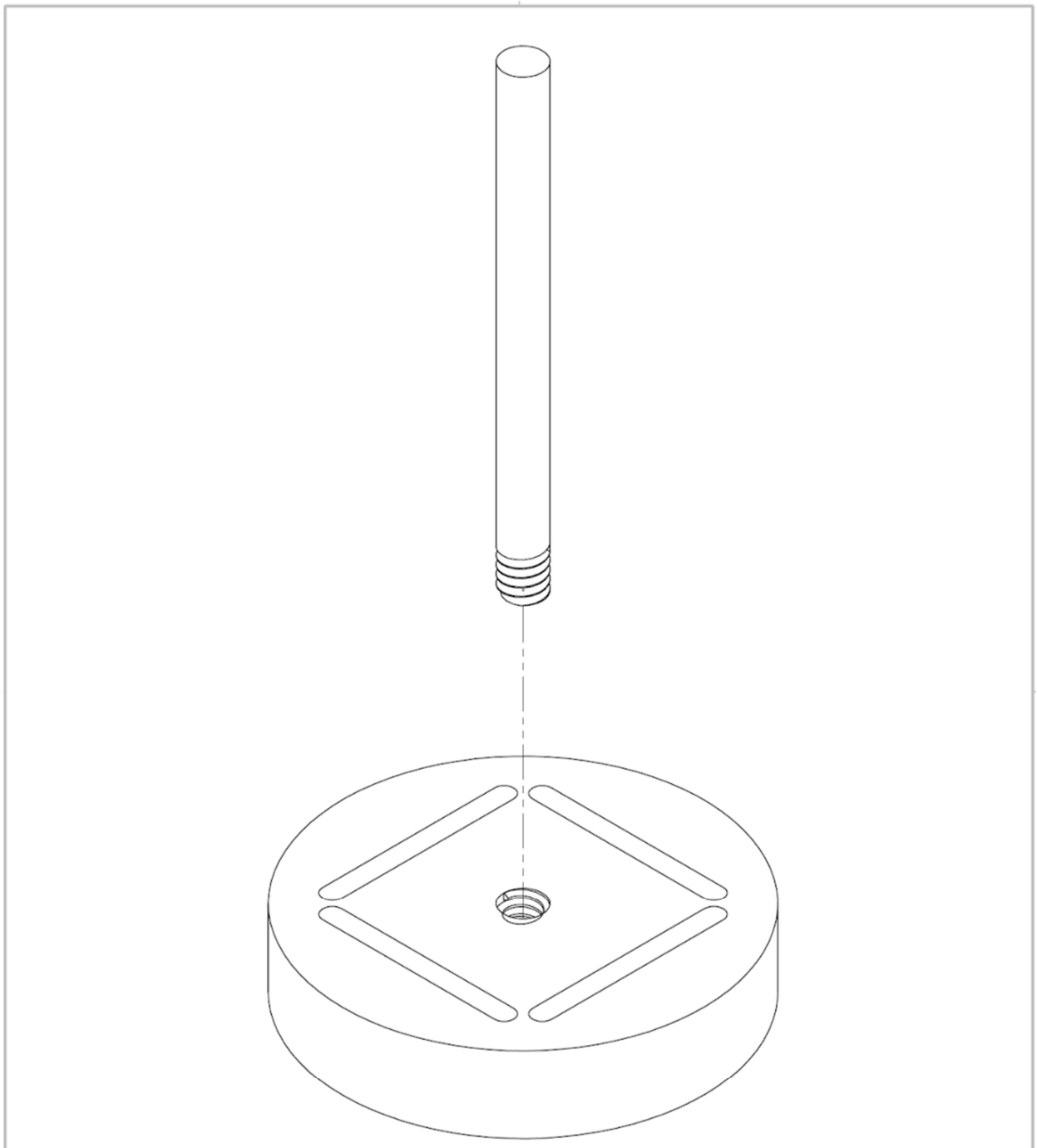

WPI

PROPRIETARY AND CONFIDENTIAL

THE INFORMATION CONTAINED IN THIS DRAWING IS THE SOLE PROPERTY OF <COMPANY NAME >. ANY REPRODUCTION IN PART OR AS A WHOLE WITHOUT THE WRITTEN PERMISSION OF <COMPANY NAME> IS PROHIBITED.

NEXT ASSY | USED ON

APPLICATION

DIMENSIONS ARE IN INCHES
TOLERANCES:
FRACTIONAL ±
ANGULAR: MACH ± BEND ±
TWO PLACE DECIMAL ±
THREE PLACE DECIMAL ±

MATERIAL PTFE

FINISH

DO NOT SCALE DRAWING

	NAME	DATE
DRAWN	L. GAGNE	11-5-2018
CHECKED		
ENG APPR.		
MFG APPR.		
Q.A.		

COMMENTS:

Worester Polytechnic Institute

FTO Plate Holder Assembly

SIZE A | DWG. NO. 10001 | REV.

SCALE:2:1 | WEIGHT: | SHEET 1 OF 1

Appendix C: Example Calculation for PCE

To calculate PCE first the Voltage data was multiplied by -1 and the current was divided by the area of the cell. For our area calculation we approximated 0.3 cm^2 for all cells. These new values can be graphed on a curve such as sample 4 below. Curves for each sample can be found in Appendix D.

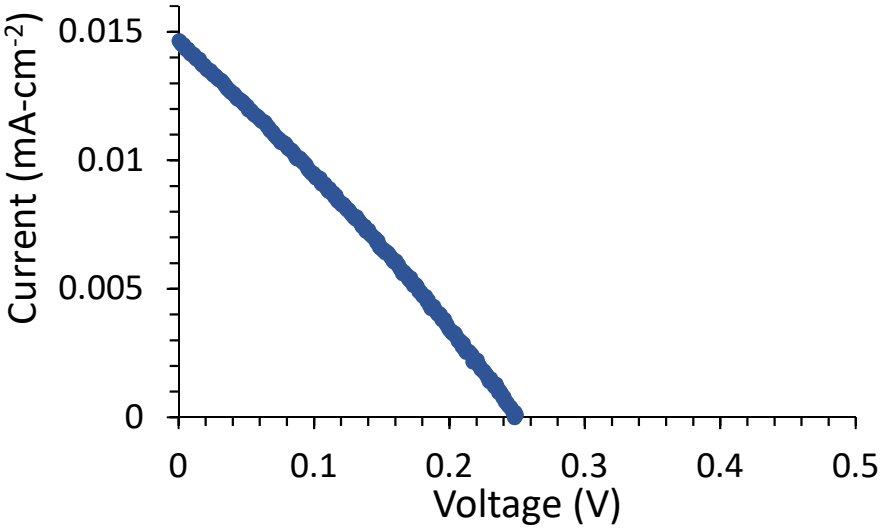

Each of these data points can then be turned to efficiency using the formula below where Voltage is in Volts, Current is in mA-cm^{-2} and the Area is in cm^2

$$\frac{Voltage * Current}{\frac{100mW}{cm^2} * Area} * 100 = \%\, efficency$$

A maximum efficiency could then be found using the Max function in excel or graphically as seen below again sample 4

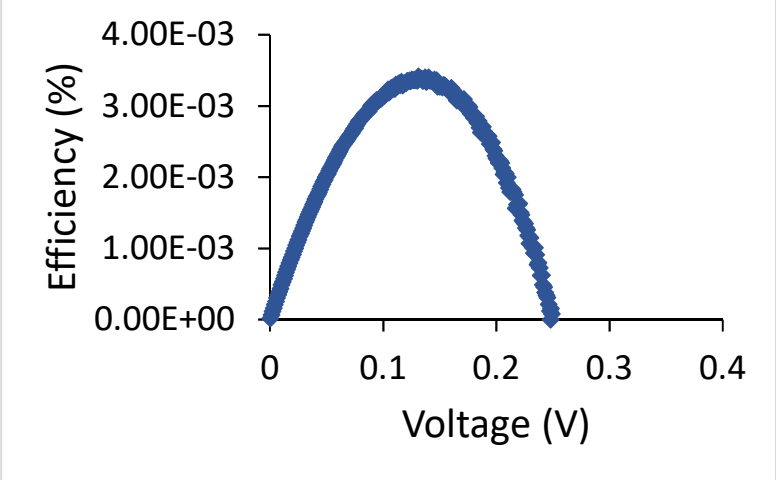

Appendix D: Photovoltaic data

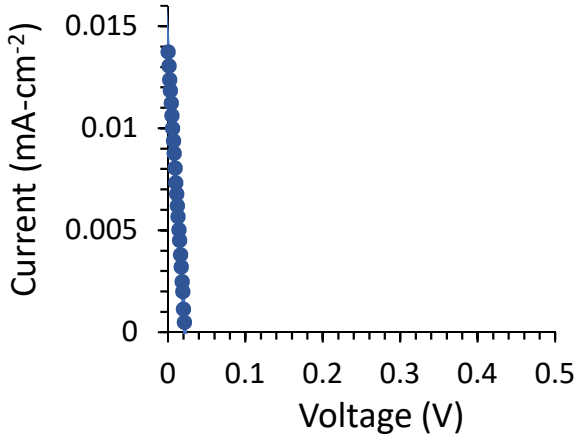

Sample 1 Efficiency 0.00025%

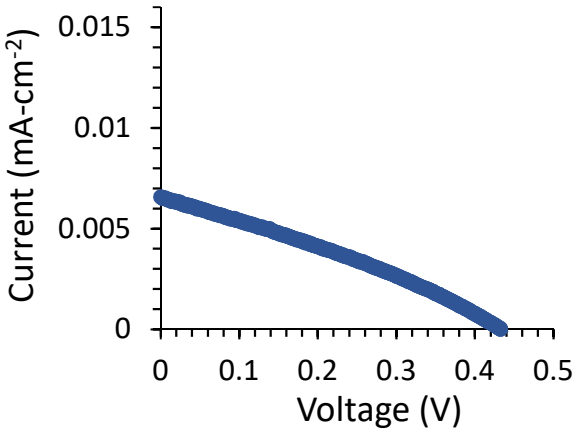

Sample 2 Efficiency 0.0029%

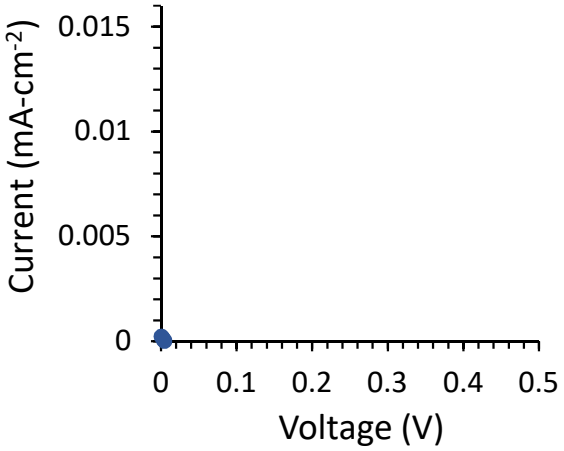

Sample 3 Efficiency 0%

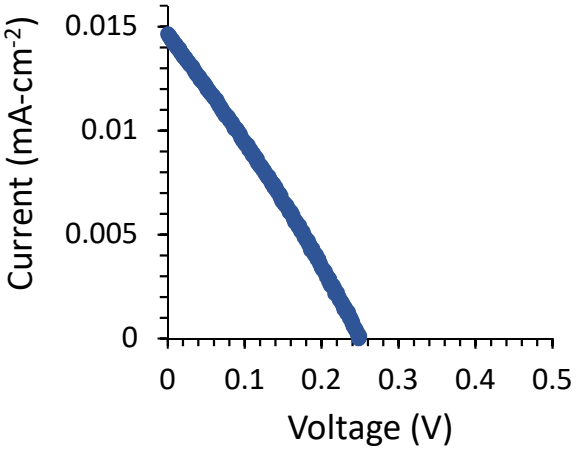

Sample 4 Efficiency 0.0034%

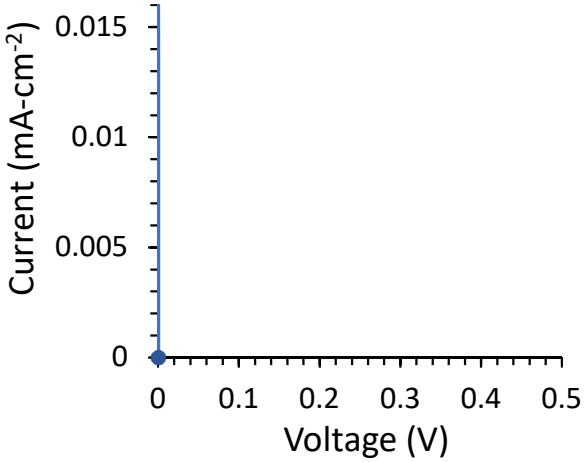

Sample 5 Efficiency 0%

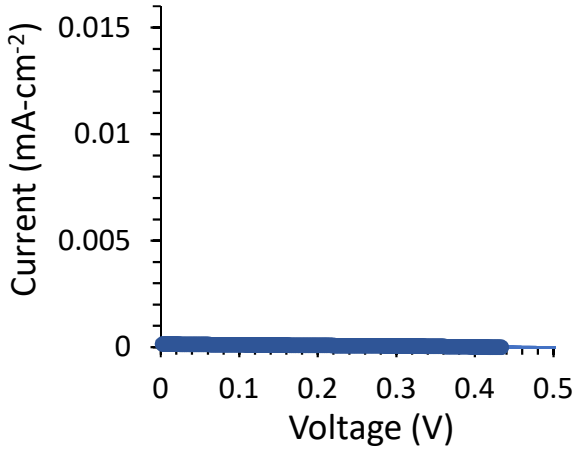

Sample 6 Efficiency 0%

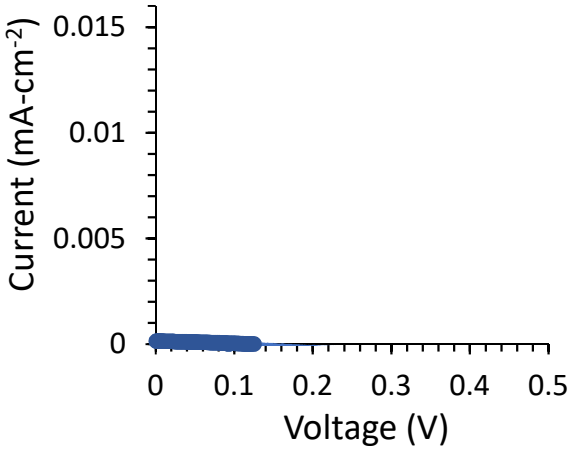

Sample 7 Efficiency 0%

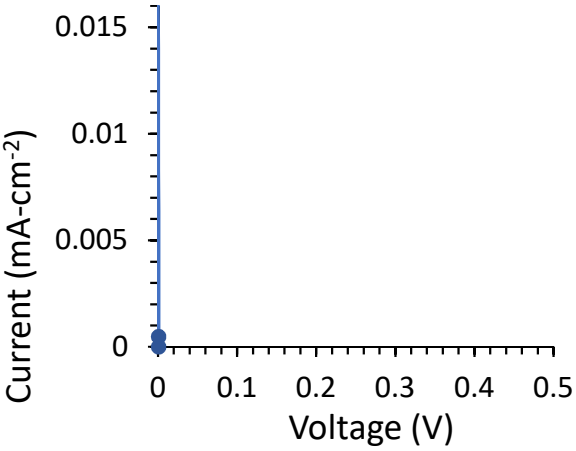

Sample 8 Efficiency 0%

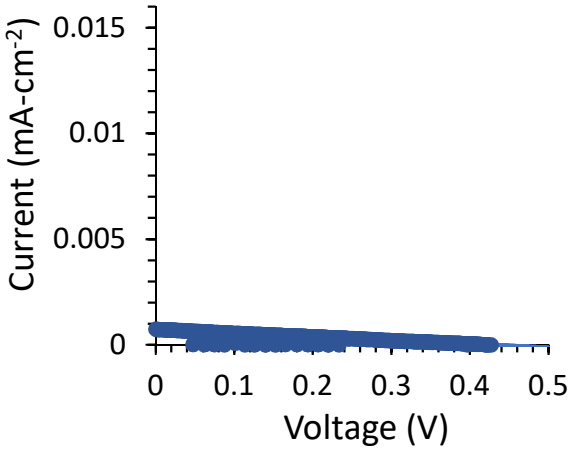

Sample 9 Efficiency 0.00026%

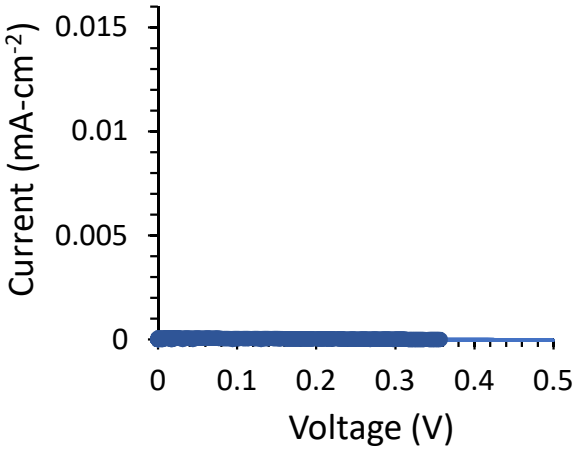

Sample 10 Efficiency 0%

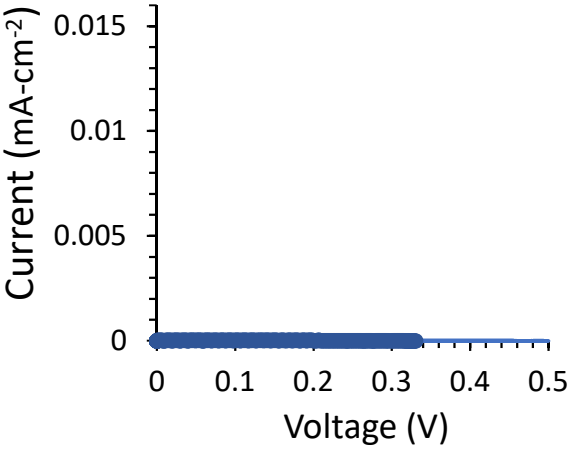

Sample 11 Efficiency 0%

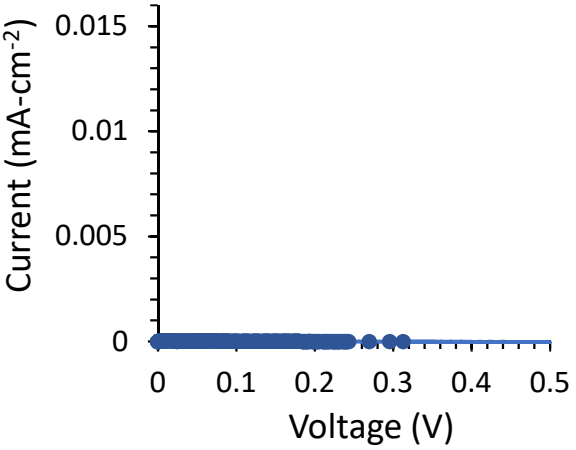

Sample 12 Efficiency 0%

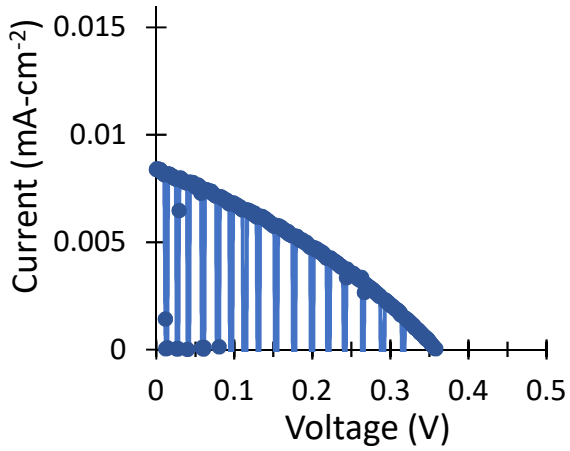

Sample 13 Efficiency 0.0032%

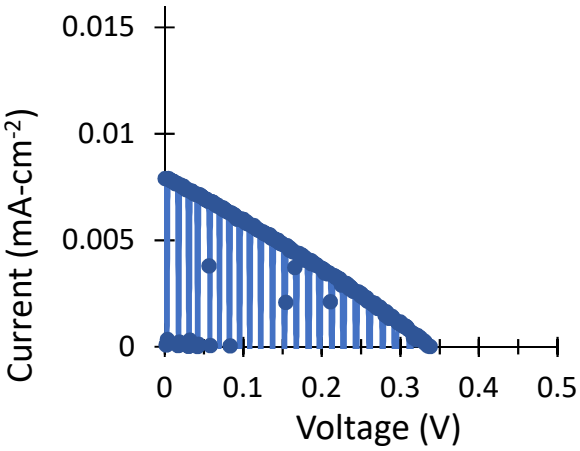

Sample 14 Efficiency 0.0025%

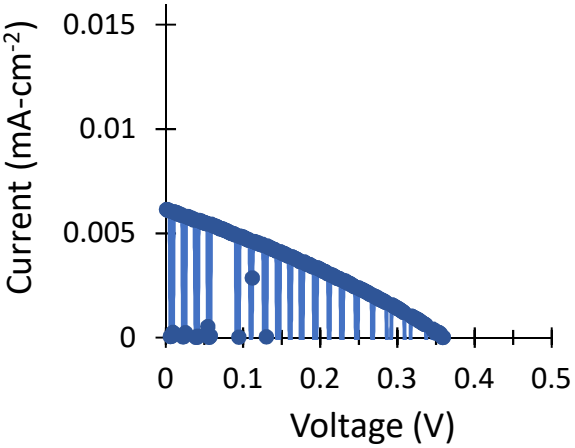

Sample 15 Efficiency 0.0022%

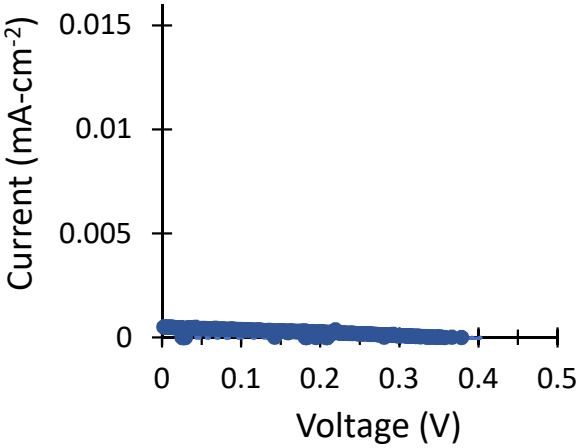

Sample 16 Efficiency 0.00018%

Appendix E: Sample Methods and Corresponding Efficiencies

Sample Number	Ratio of TiO_2 Paste/Ethanol (w/w)	m-TiO_2 Particle Diameter	CuSCN Method	TiO_2 Application Method	Layers	Max PCE (%)
1	50/50	20nm	2	Spin Coated	2	0.00025
2	50/50	20nm	2	Spin Coated	1	0.0029
3	50/50	20nm	1	Spin Coated	2	0
4	50/50	20nm	1	Spin Coated	1	0.0034
5	50/50	20nm	1	Spin Coated	1	0
6	50/50	20nm	1	Spin Coated	2	0
7	50/50	20nm	1	Spin Coated	3	0
8	50/50	20nm	1	Doctor Bladed	1	0
9	50/50	20nm	3	Spin Coated	1	0.00026
10	50/50	20nm	3	Spin Coated	2	0
11	50/50	20nm	3	Spin Coated	3	0
12	50/50	20nm	3	Doctor Bladed	1	0
13	20/80	22nm and >150nm	3	Spin Coated	1	0.0032
14	50/50	22nm and >150nm	3	Spin Coated	1	0.0025
15	20/80	22nm and >150nm	3	Doctor Bladed	1	0.0022
16	50/50	22nm and >150nm	3	Doctor Bladed	1	0

Appendix F: SEM Images of Samples 1 and 2

Sample 1 Before CQDs

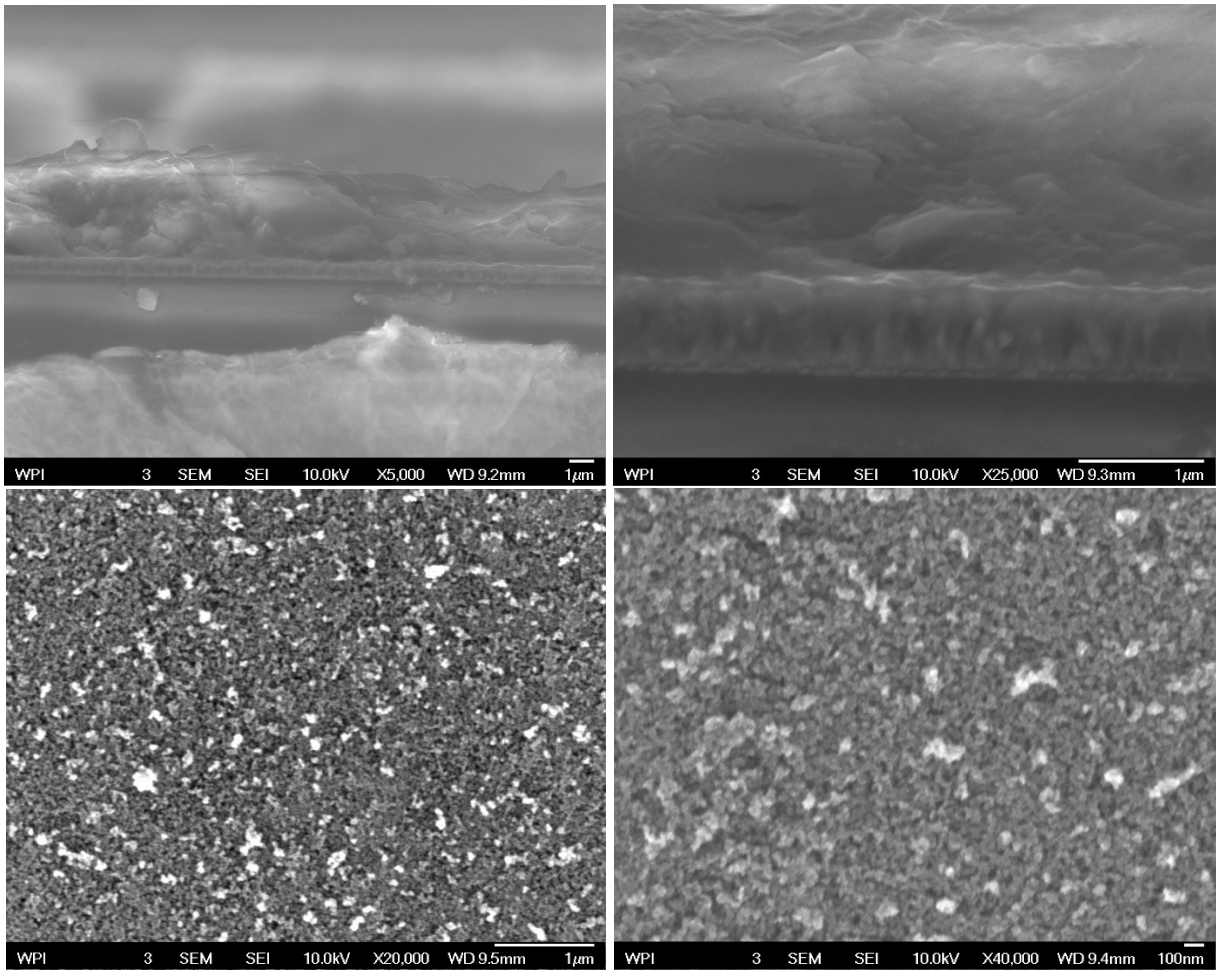

Sample 1 After CQDs

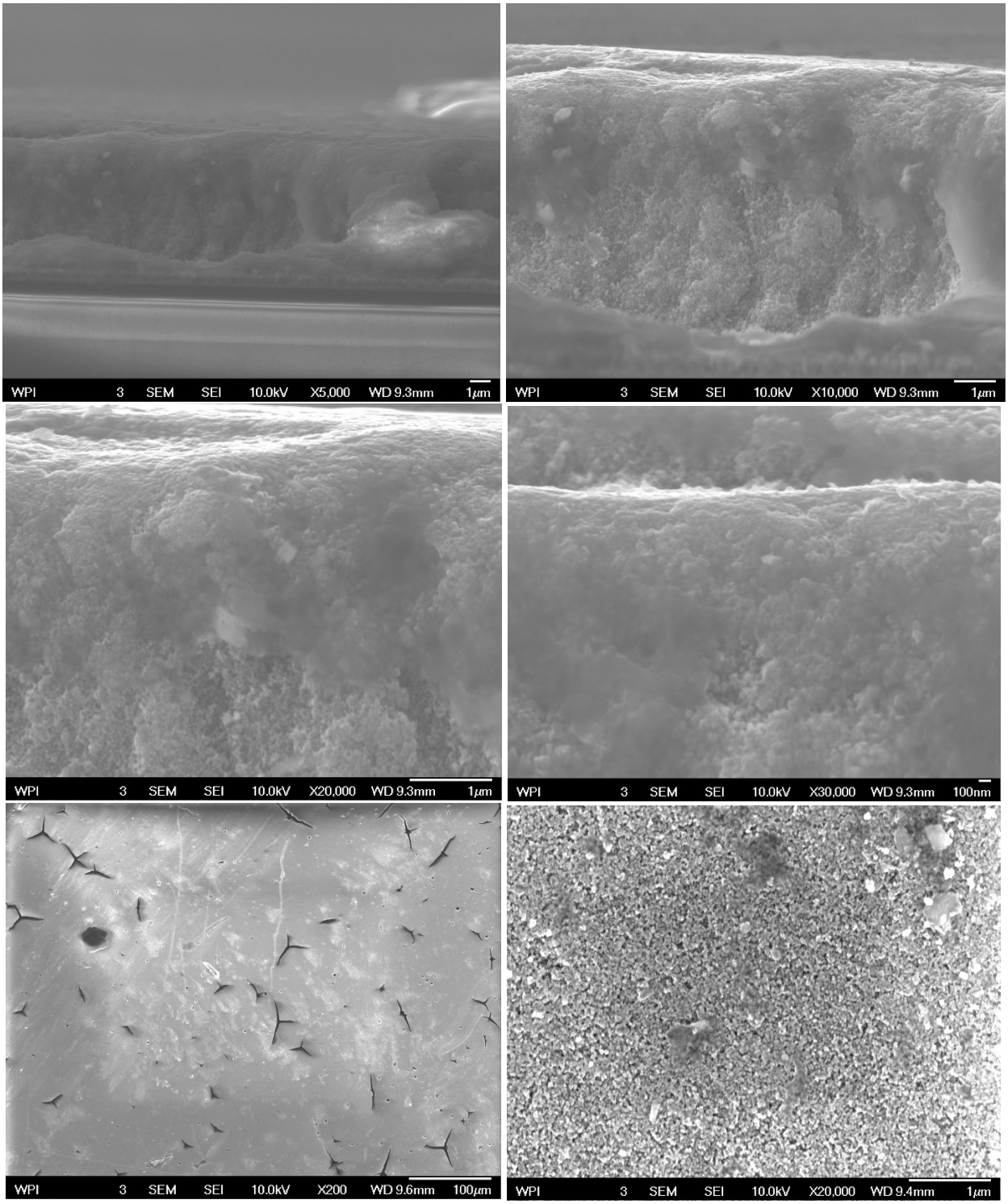

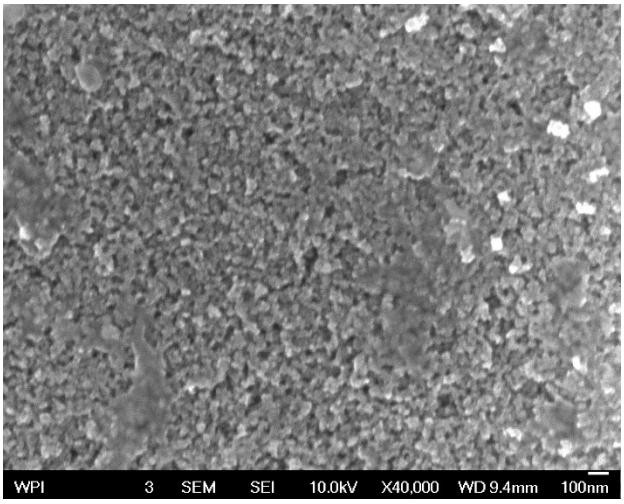

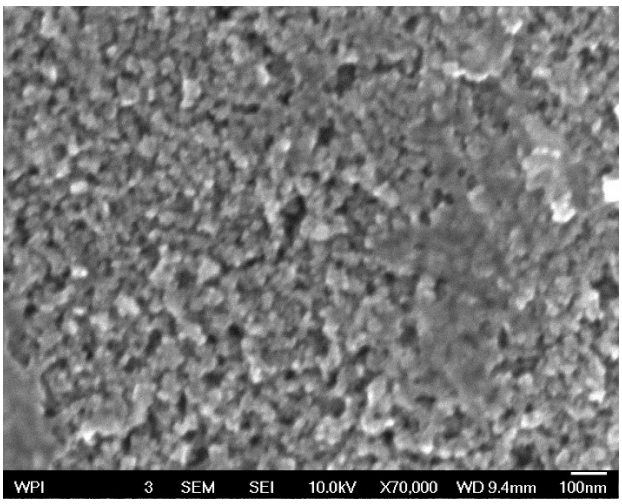

Sample 2 Before CQDs

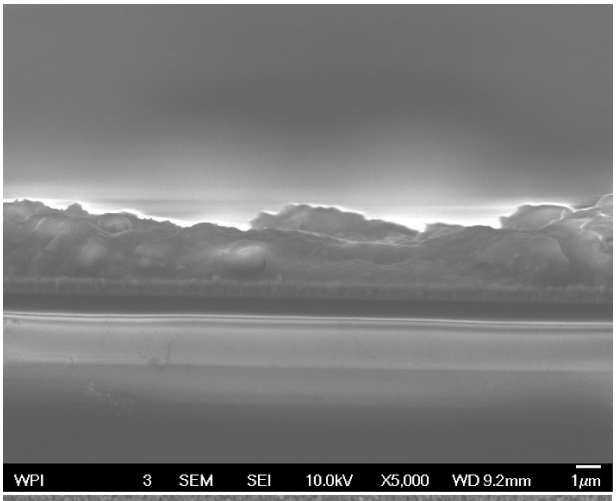

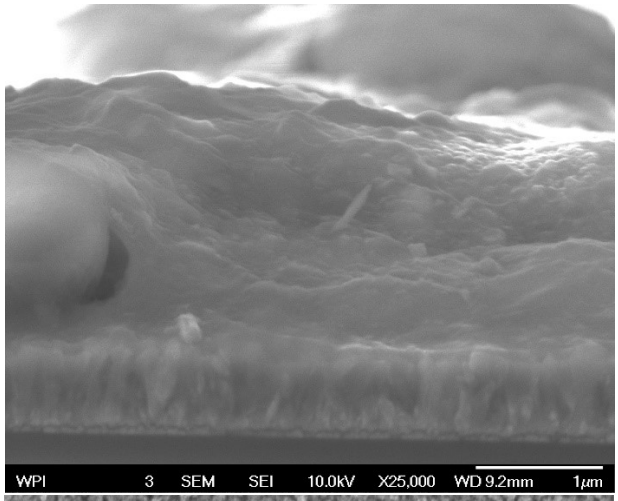

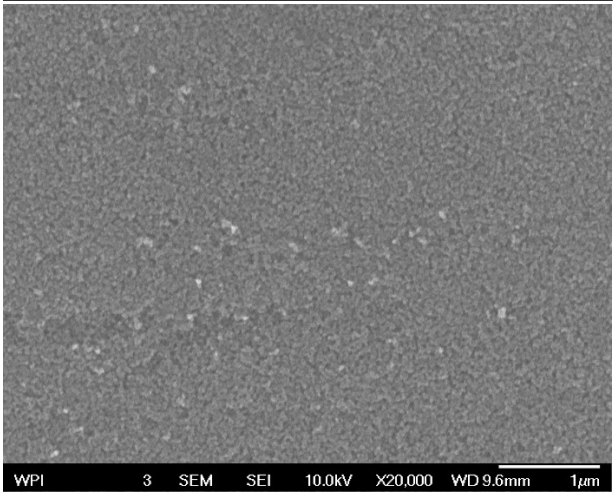

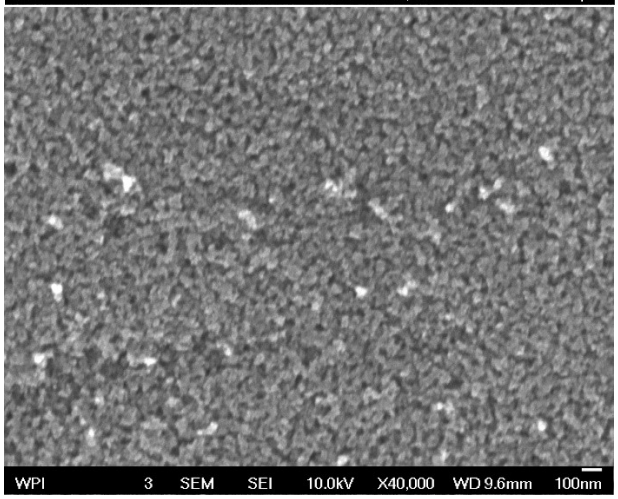

Sample 2 After CQDs